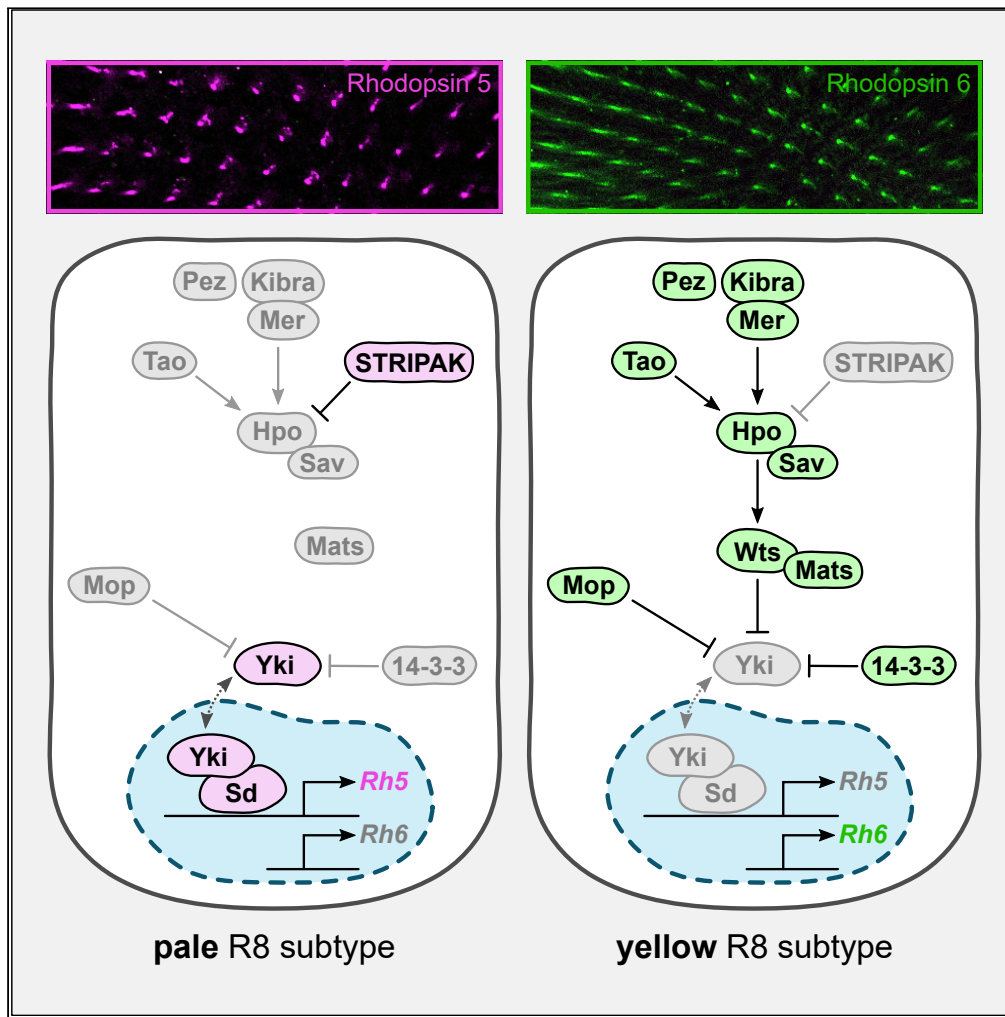


Article

The Hippo pathway uses different machinery to control cell fate and organ size



Jonathan M. Pojer,  
Samuel A.  
Manning,  
Benjamin Kroeger,  
Shu Kondo, Kieran  
F. Harvey

kieran.harvey@petermac.org

Highlights

A subset of Hippo pathway proteins control the fate of R8 photoreceptor neurons

Hippo pathway proteins are mostly cytoplasmic, not junctional, in R8 cells

Hippo pathway proteins are expressed higher in the growth phase of eye development



## Article

## The Hippo pathway uses different machinery to control cell fate and organ size

Jonathan M. Pojer,<sup>1,2</sup> Samuel A. Manning,<sup>1,3</sup> Benjamin Kroeger,<sup>1,3</sup> Shu Kondo,<sup>4</sup> and Kieran F. Harvey<sup>1,2,3,5,\*</sup>

## SUMMARY

**The Hippo pathway is a conserved signaling network that regulates organ growth and cell fate. One such cell fate decision is that of R8 photoreceptor cells in the *Drosophila* eye, where Hippo specifies whether cells sense blue or green light. We show that only a subset of proteins that control organ growth via the Hippo pathway also regulate R8 cell fate choice, including the STRIPAK complex, Tao, Pez, and 14-3-3 proteins. Furthermore, key Hippo pathway proteins were primarily cytoplasmic in R8 cells rather than localized to specific membrane domains, as in cells of growing epithelial organs. Additionally, Warts was the only Hippo pathway protein to be differentially expressed between R8 subtypes, while central Hippo pathway proteins were expressed at dramatically lower levels in adult and pupal eyes than in growing larval eyes. Therefore, we reveal several important differences in Hippo signaling in the contexts of organ growth and cell fate.**

## INTRODUCTION

The Hippo pathway is an important regulator of organ size, integrating signals from surrounding cells, the extracellular matrix, and mechanical forces to control cell proliferation and apoptosis (Gaspar and Tapon, 2014; Irvine and Harvey, 2015; Schroeder and Halder, 2012; Zheng and Pan, 2019). There have been more than 40 proteins that have been associated with the Hippo pathway (Figure 1A), and deregulation of this pathway has been linked to the formation of multiple cancers (Harvey et al., 2013; Kulkarni et al., 2020). The central unit of the pathway is a kinase cassette (Figure 1A'), composed of the sterile-20-like (Ste20) kinase, Hippo (Hpo) (Harvey et al., 2003; Jia et al., 2003; Pantalacci et al., 2003; Udan et al., 2003; Wu et al., 2003), the nuclear DBF2-related (NDR) kinase, Warts (Wts) (Justice et al., 1995; Tapon et al., 2002; Xu et al., 1995), and the scaffold factors, Salvador (Sav) (Kango-Singh et al., 2002; Tapon et al., 2002) and Mob as tumor suppressor (Mats) (Lai et al., 2005). Hpo phosphorylates and activates Wts, which phosphorylates and suppresses the activity of the transcriptional coactivator, Yorkie (Yki) (Gaspar and Tapon, 2014; Irvine and Harvey, 2015; Schroeder and Halder, 2012; Zheng and Pan, 2019) (Figures 1A–1A'). Yki is the key transcriptional activator of the Hippo pathway; however, it cannot bind to DNA itself. To regulate gene expression, Yki associates with transcription factors, primarily the TEAD/TEF transcription factor, Scalloped (Sd) (Goulev et al., 2008; Wu et al., 2008; Zhang et al., 2008). Phosphorylated Yki interacts with the *D. melanogaster* 14-3-3 protein orthologs, 14-3-3e and 14-3-3ζ, leading to increased cytoplasmic localization and reduced transcriptional activity (Ren et al., 2010). Several proteins regulate the Hippo pathway upstream of the core kinase cassette (Figure 1A), including the WW domain protein, Kibra (Baumgartner et al., 2010; Genevet et al., 2010; Yu et al., 2008); the 4.1/ezrin/radixin/moesin (FERM) domain proteins, Merlin (Mer), Expanded (Ex), and Pez (Hamaratoglu et al., 2006; Poernbacher et al., 2012); the Ste20 kinase, Tao (Boggiano et al., 2011; Poon et al., 2011), and the STRIPAK components, Connector of kinase to AP-1 (Cka), Microtubule star (Mts), Slmap, and Rassf (Ribeiro et al., 2010; Zheng et al., 2017).

Although the Hippo pathway was first identified as a regulator of organ growth, it also controls several cell fate decisions, such as R8 photoreceptor subtypes in the *D. melanogaster* eye (Jukam et al., 2013; Jukam and Desplan, 2011; Mikeladze-Dvali et al., 2005). The R8 photoreceptor cell is one of eight photosensitive cell types found in the subunits of the *D. melanogaster* eye, called ommatidia. Each photoreceptor cell has a specialized subcellular compartment composed of tens of thousands of microvilli, called the rhabdome, which projects into the space at the center of each ommatidium. The rhabdomeres of the R8 cell and the neighboring R7 cell share the same optic path, with the R8 cell located proximally (Figures 1B–1B') (Ready, 2002). Each photoreceptor cell expresses a specific photosensitive G protein-coupled receptor, which has a distinct spectral sensitivity (known as rhodopsins), allowing each cell to respond to a

<sup>1</sup>Peter MacCallum Cancer Centre, 305 Grattan St, Melbourne, VIC 3000, Australia

<sup>2</sup>Sir Peter MacCallum Department of Oncology, The University of Melbourne, Parkville, VIC 3010, Australia

<sup>3</sup>Department of Anatomy and Developmental Biology, Monash University, Clayton, VIC 3800, Australia

<sup>4</sup>Laboratory of Invertebrate Genetics, National Institute of Genetics, 1111 Yata, Mishima, Shizuoka, Japan

<sup>5</sup>Lead contact

\*Correspondence: kieran.harvey@petermac.org  
<https://doi.org/10.1016/j.isci.2021.102830>



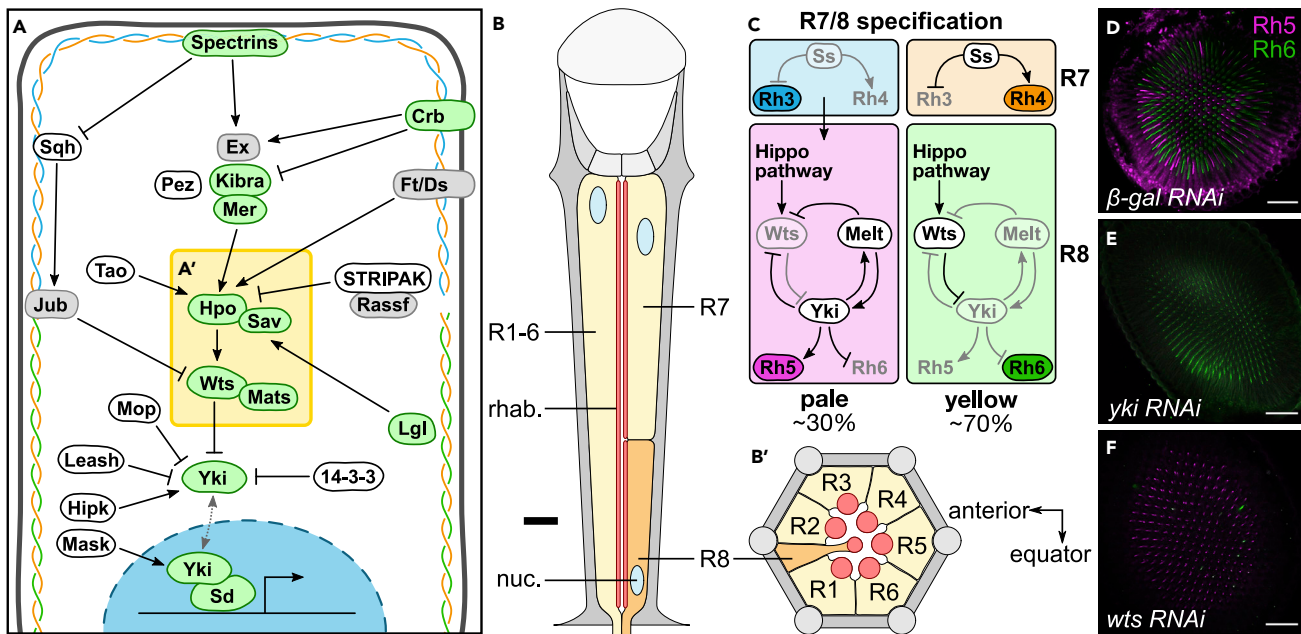


**Figure 1. Regulation of *Drosophila melanogaster* R8 cell fate by the Hippo pathway**

(A and A') Schematic of the Hippo pathway in tissue growth. Proteins labeled in green have already been shown to play a role in R8 cell fate; proteins labeled in gray have already been shown to not play a role in R8 cell fate; proteins labeled in white have not been studied in R8 cell fate. The core kinase cassette is shown in the yellow box (A'). Crb, Crumbs; Ds, Dachshous; Ex, Expanded; Ft, Fat; Hpo, Hippo; Jub, Ajuba; Lgl, Lethal (2) giant larvae; Mats, Mob as tumor suppressor; Mer, Merlin; Mop, Myopic; Rassf, Ras association family member; Sav, Salvador; Sd, Scalloped; STRIPAK, Striatin-interacting phosphatase and kinase; Sqh, Spaghetti squash; Wts, Warts; Yki, Yorkie.

(B and B') Schematic diagram of a *Drosophila* ommatidium. Yellow cells are R1-7 photoreceptor cells; orange cells are R8 photoreceptor cells; gray cells are other cells in the ommatidium. Blue circles are photoreceptor nuclei (nuc.); red lines/circles are rhabdomeres (rhab.). (B) Longitudinal section of an ommatidium. Note that R7 and R8 cells share the same optic path. The thick black line indicates where the transverse section (B') is drawn from. The distal section of the retina (toward the lens and outer surface of the eye) is to the top; the proximal section of the retina (toward the brain) is to the bottom. (B') Transverse section of the proximal section of an ommatidium, showing the R8 cell. The anterior of the retina is to the left; the equator of the retina is to the bottom.

(C) The main photoreceptor subtypes, showing R7 and R8 cell specification in each subtype. In the pale subtype, the R7 cell expresses *Rh3* (blue), signaling to the R8 cell to take on a pR8 cell fate through a bistable loop composed of Warts (Wts), Melted (Melt), and Yorkie (Yki) and promoting expression of *Rh5* (magenta). In the yellow subtype, the R7 cell expresses *spineless* (*ss*), which promotes *Rh4* (orange), while the R8 cell expresses *Rh6* (green). The subtypes are found in the specified proportions.

(D–F) Confocal microscope images of adult *Drosophila* retinas stained with anti-Rh5 (magenta) and anti-Rh6 (green) antibodies. All lines were driven by *IGMR-Gal4*. Retinas expressing *β-gal RNAi* had a wild-type ratio of R8 subtypes (C); retinas expressing *yki RNAi* had nearly only pR8 cells (D); retinas expressing *wts RNAi* had nearly only yR8 cells (E). Scale bars are 50 μm.

specific range of wavelengths of light (Schnaitmann et al., 2013; Sharkey et al., 2020). The R7 and R8 cells mediate color vision and can express one of *Rhodopsin 3* (*Rh3*), *Rh4*, *Rh5*, or *Rh6* (Yamaguchi et al., 2010); the rhodopsin expressed in each cell is determined by the subtype of ommatidium.

The two main subtypes of ommatidia are known as the “pale” (p) and “yellow” (y) subtypes, which make up around 30% and 70% of all ommatidia, respectively. In the p subtype, pR7 cells express the short UV-sensitive *Rh3*, whereas pR8 cells express the blue-sensitive *Rh5*. In the y subtype, yR7 cells express the long UV-sensitive *Rh4* and yR8 cells express the green-sensitive *Rh6* (Figure 1C). Specification of R7 and R8 cells begins in the late pupal retina, where the transcription factor, Spineless, is stochastically expressed in a subset of R7 cells that develop into yR7 cells, with the remaining R7 cells taking on a pR7 cell fate (Johnston and Desplan, 2014; Wernet et al., 2006). In pR7 cells, a signal conveyed by the transforming growth factor β pathway instructs the neighboring R8 cells to become pR8 cells (Figure 1C) (Wells et al., 2017).

The fate of R8 cells is controlled by a bistable feedback loop composed of Wts, Yki, and the Pleckstrin-homology domain protein Melted (Melt) (Jukam et al., 2013; Mikeladze-Dvali et al., 2005). In pR8 cells, Yki is active and can promote expression of *Rh5* and its activator, *melt*, while it suppresses transcription of its repressor, *wts*. In yR8 cells, Wts is active and limits Yki activity, thereby preventing the pR8 cell fate and

allowing expression of *Rh6* (Jukam et al., 2013; Xie et al., 2019) (Figures 1C–1F). The Hippo pathway is also essential for the maintenance of R8 cell fate in adult *D. melanogaster* eyes, ensuring that only one rhodopsin is expressed in each R8 cell and preventing sensory overlap (Jukam and Desplan, 2011). Interestingly, although the Hippo pathway core kinase cassette, Yki and Sd control both organ growth and R8 cell fate, not all Hippo pathway members do so. For example, Ex; the planar polarity regulators, Fat and Dachous; and the mechanosensors  $\beta$ -Spectrin and Ajuba (Jub) do not regulate R8 cell fate choice (Jukam and Desplan, 2011; Pojer et al., 2021) (Figure 1A). Currently, however, we lack a complete understanding of which Hippo pathway proteins that regulate organ growth also participate in the R8 cell fate choice.

In epithelial cells of growing organs like the larval eye and wing imaginal discs, Hippo pathway activity is regulated by recruitment of different proteins to specialized membrane subdomains. The majority of Wts resides at adherens junctions where it is held in an inactive complex with Jub (Rauskolb et al., 2014). Wts is thought to be activated by Hpo when it is recruited to the sub-apical region and the medial apical membrane, where it forms complexes with Ex, Mer, and Kibra (Su et al., 2017; Sun et al., 2015). R8 cells have highly specialized apical membrane domains, which comprise the rhabdomere and stalk membrane, but whether Hippo pathway proteins are regulated by recruitment to these membranes in R8 cells is unknown.

Here, we conducted a select screen to identify new regulators of R8 cell fate and also investigated the sub-cellular localization of Hippo pathway proteins in R8 cells in both pupal and adult eyes. We identified a number of new regulators of R8 cell fate, including the STRIPAK complex, Tao, Pez, 14-3-3 $\epsilon$ , and 14-3-3 $\zeta$ . We also found that Hippo pathway proteins are expressed at dramatically lower levels in pupal and adult eyes than in larval eye imaginal discs but were largely cytoplasmic, as opposed to enriched in particular membrane domains, as in cells of growing epithelial organs. Furthermore, Wts is the only Hippo pathway protein to obviously differ in expression levels between R8 subtypes.

## RESULTS

To further investigate the role of the Hippo pathway in R8 cell fate specification, we assessed the effect of genetically depleting Hippo pathway proteins on R8 cell fate. Mutations in genes that are Hippo pathway repressors/Yki promoters compromise cell viability and proliferation in growing mosaic tissues. Therefore, we used the *long Glass Multiple Reporter (IGMR)-Gal4* driver (Wernet et al., 2003) to drive RNAi lines in all photoreceptor cells to investigate the roles of these genes in R8 cell fate while minimizing other phenotypes that affect eye and photoreceptor development. The ratio of R8 subtypes was examined by analyzing the ratio of R8 cells expressing Rh5 or Rh6, relative to control eyes (Figure 1D,  *$\beta$ -gal RNAi*, which was approximately 30% pR8 cells, consistent with previous studies [Jukam and Desplan, 2011; Mikeladze-Dvali et al., 2005]). We assessed the roles of components of the STRIPAK phosphatase complex, *Tao*, *Pez*, 14-3-3 $\epsilon$ , 14-3-3 $\zeta$ , *mask*, *Hipk*, *myopic (mop)*, and *leash*.

### The STRIPAK phosphatase complex promotes pR8 cell fate while Tao and Pez promote yR8 cell fate

Hpo is the upstream kinase in the Hippo pathway core kinase cassette and is repressed by the STRIPAK PP2A phosphatase complex, which inactivates Hpo by dephosphorylating its activation loop motif (Ribeiro et al., 2010). Two key components of the STRIPAK complex are the striatin homologue, *Cka*, and the PP2A C subunit, *Mts* (Ribeiro et al., 2010). Other important STRIPAK members include the adaptor proteins *Rassf* and *Slmap*, which link the STRIPAK complex to Hpo (Ribeiro et al., 2010; Zheng et al., 2017). Although *Rassf* does not regulate R8 cell fate (Jukam and Desplan, 2011), the STRIPAK complex may still regulate Hpo in R8 cells via a different adaptor protein. Depletion of *Cka* (0%–4% pR8 cells across three RNAi lines,  $p < 0.001$ ) and *mts* (approximately 12% pR8 cells,  $p < 0.001$ ) both caused a strong increase in the proportion of yR8 cells (Figures 2A, 2B, 2D, S1A, and S1B). Surprisingly, depletion of *Slmap* did not alter the ratio of R8 subtypes (23%–26% pR8 cells across 2 RNAi lines,  $p > 0.032$ ), suggesting that it does not regulate R8 cell fate, or does so in a redundant fashion with another adaptor STRIPAK protein such as *Rassf* (Figures 2C, 2D and S1C). To test the second hypothesis, we expressed *Slmap RNAi* in conjunction with either  *$\beta$ -gal RNAi* or *Rassf RNAi* and observed similar phenotypes (around 22% pR8 cells for both,  $p = 0.86$ ) (Figures S2A, S1B, and S1E). These results indicate that the core components of the STRIPAK complex, *Cka* and *Mts*, do indeed regulate R8 cell fate, whereas *Slmap* does not.

In the context of epithelial organ growth and neural stem cell proliferation, Hpo is also regulated by the Ste20 kinase, *Tao*, which promotes Hpo activity by phosphorylating its activation loop motif (Boggiano

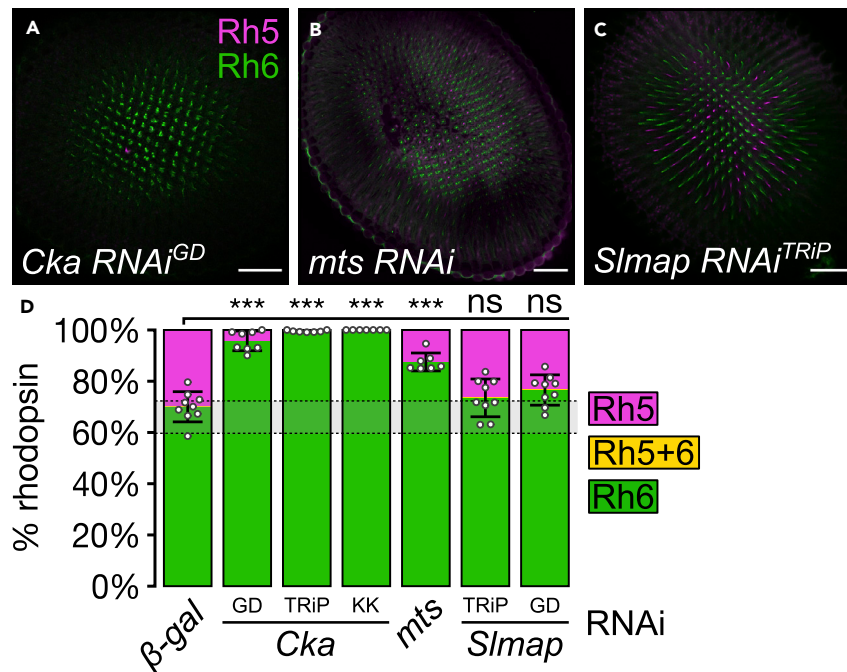


**Figure 2. The STRIPAK complex promotes pR8 cell fate**

(A–C) Confocal microscope images of adult *Drosophila* retinas stained with anti-Rh5 (magenta) and anti-Rh6 (green) antibodies. All lines were driven by *IGMR-Gal4*. Retinas expressed *Cka* RNAi<sup>GD</sup> (A), *mts* RNAi (B), and *Slmap* RNAi<sup>TRIP</sup> (C). Scale bars are 50  $\mu$ m.

(D) Proportion of R8 cells that express Rh5 (magenta), Rh6 (green), or both (yellow). The error bars represent the standard deviation of total % Rh5 (% Rh5 + % Rh5+Rh6). Total % Rh5 was compared with two-sided, unpaired t test; ns, not significant, \*\*\*p < 0.0001. The shaded gray region between the dotted gray lines indicates wild-type Rh5:Rh6 ratio range. Error bars are  $\pm$  SD.  $\beta$ -gal RNAi (Figure 1D): n = 9 retinas, 3,976 ommatidia; *Cka* RNAi<sup>GD</sup>: n = 7, 1,071; *Cka* RNAi<sup>TRIP</sup>: n = 8, 1,637; *Cka* RNAi<sup>KK</sup>: n = 7, 1,240; *mts* RNAi: n = 7, 2,920; *Slmap* RNAi<sup>TRIP</sup>: n = 9, 2,173; *Slmap* RNAi<sup>GD</sup>: n = 9, 2,361. See also Figures S1 and S2.

et al., 2011; Poon et al, 2011, 2016). To determine whether Tao regulates R8 cell fate, we depleted it in photoreceptor cells, which resulted in a moderate increase in the proportion of pR8 cells (approximately 39% pR8 cells, p = 0.0007) (Figures 3A and 3E). Consistent with this, expression of a hyperactive *Tao* transgene caused all R8 cells to adopt the yR8 fate (0% pR8 cells, p < 0.0001) (Figures 3B, 3C, and 3E), arguing that *Tao* has a minor role in regulating Hippo pathway activity in R8 cells. As *Tao* and the STRIPAK complex both regulate activation loop phosphorylation of Hpo, we depleted *Tao* simultaneously with *mts* and found that the R8 ratio was similar to when *mts* was depleted alone (approximately 10% and 6% pR8 cells, respectively; p = 0.011) (Figures S2C–S2E). These results are consistent with a scenario where *Tao* and the STRIPAK complex act in parallel to control Hippo phosphorylation and activity, and where the loss of *Tao* cannot overcome Hpo hyperactivation caused by the loss of STRIPAK.

Pez is a FERM domain protein that interacts with Kibra to restrict Yki activity in intestinal stem cells (Poernbacher et al., 2012). As Kibra is essential for yR8 cell fate specification (Jukam and Desplan, 2011), we investigated whether Pez is also required for the yR8 cell fate. Depletion of Pez led to a moderate increase in the proportion of pR8 cells (approximately 47% pR8 cells, p < 0.0001) (Figures 3D and 3E), consistent with a minor role for Pez as a Yki repressor in R8 cells.

### The 14-3-3 proteins, Mask, and Myopic promote yR8 cell fate

We also investigated proteins that interact with the central Hippo pathway effector, Yki, including the 14-3-3 proteins, Mask, Mop, Leash, and Hipk. The *D. melanogaster* 14-3-3 proteins, 14-3-3e and 14-3-3z, bind to Yki and promote its localization in the cytoplasm (Ren et al., 2010). Depletion of 14-3-3e in photoreceptor cells causes a partial transition to the pR8 fate (around 59% pR8 cells, p < 0.0001), whereas depletion of 14-3-3z did not alter the ratio of R8 subtypes (approximately 30% pR8 cells, p = 0.91) (Figures 4A, 4B, and 4H).

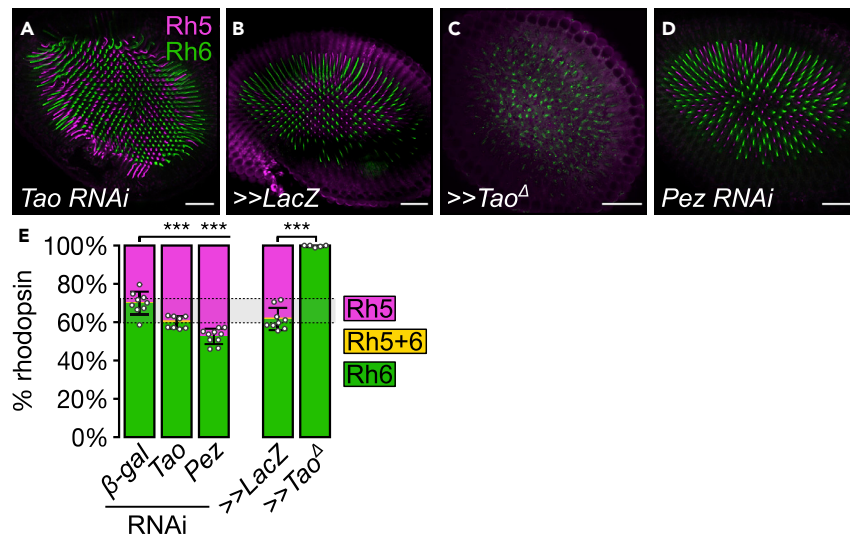


**Figure 3. Tao and Pez promote yR8 cell fate**

(A–D) Confocal microscope images of adult *Drosophila* retinas stained with anti-Rh5 (magenta) and anti-Rh6 (green) antibodies. All lines were driven by *IGMR-Gal4*. Retinas expressed *Tao RNAi* (A), *LacZ* (B), *Tao $\Delta$*  (C), and *Pez RNAi* (D). Scale bars are 50  $\mu$ m.

(E) Proportion of R8 cells that express Rh5 (magenta), Rh6 (green), or both (yellow). The error bars represent the standard deviation of total % Rh5 (% Rh5 + % Rh5+Rh6). Total % Rh5 was compared with two-sided, unpaired t test; ns, not significant, \*\*p < 0.001, \*\*\*p < 0.0001. The shaded gray region between the dotted gray lines indicates wild-type Rh5:Rh6 ratio range. Error bars are +/- SD.  $\beta$ -gal RNAi (Figure 1D): n = 9 retinas, 3,976 ommatidia; *Tao RNAi*: n = 8, 3,925; *Pez RNAi*: n = 10, 2,386; >>*LacZ*: n = 9, 3,211; >>*Tao $\Delta$* : n = 5, 837.

As 14-3-3 proteins can function redundantly (Acevedo et al., 2007), we depleted both 14-3-3 $\epsilon$  and 14-3-3 $\zeta$ , which resulted in nearly all photoreceptors adopting the pR8 cell fate (on average 97% pR8 cells, p < 0.0001) (Figures 4C and 4H). This indicates that 14-3-3 proteins limit Yki activity in R8 cells in a partially redundant fashion.

Mop and Leash also suppress Yki activity—Mop promotes endosomal trafficking of Yki (Gilbert et al., 2011), whereas Leash recruits Yki for lysosomal degradation (Kwon et al., 2013). Conversely, both Mask, an ankyrin and KH domain-containing protein that binds to Yki, and Hipk, a serine/threonine kinase, promote Yki activity in the context of epithelial tissue growth (Chen and Verheyen, 2012; Poon et al., 2012; Sansores-Garcia et al., 2013; Sidor et al., 2013). Depletion of *mask* (39%–44% pR8 cells across two RNAi lines, p < 0.0023) and *mop* (around 39% pR8 cells, p = 0.0026) mildly increased the proportion of pR8 cells, whereas depletion of *leash* (approximately 38% pR8 cells across two RNAi lines, p = 0.012) and *hipk* (23%–32% pR8 cells across two RNAi lines, p > 0.10) did not affect the ratio of R8 subtypes (Figures 4D–4H and S1D–S1F). Therefore, the STRIPAK complex, Tao, Pez, 14-3-3 $\epsilon$ , 14-3-3 $\zeta$ , Mask, and Mop influence R8 cell fate to differing degrees, whereas Slimp, Leash, and Hipk do not appear to. Unexpectedly, depletion of *mask* showed the opposite phenotype of what was expected from its role in promoting transcription of Yki target genes in growing organs (Sansores-Garcia et al., 2013; Sidor et al., 2013). These data are consistent with previous studies that found that only a subset of Hippo pathway proteins that control Yki activity in the context of organ growth modulate R8 cell fate (Jukam and Desplan, 2011; Pojer et al., 2021).

### Expression of key Hippo pathway proteins is downregulated following the cessation of organ growth

To investigate the expression and subcellular localization of Hippo pathway proteins in photoreceptor cells, we used CRISPR-Cas9 genome editing to endogenously tag Hpo, Wts, Mer, Tao, and Kibra with the fluorescent protein Venus (Figures S3A and S3B) (Pojer et al., 2021; Poon et al., 2016). All of these strains were homozygous viable and fertile, and most displayed normal R8 subtype ratios (Figures S3C–S3G), confirming that the addition of the Venus tag did not substantially alter the function of these proteins. The Wts-Venus strain had a slight decrease in the proportion of pR8 cells (p = 0.003) (Figures S3D–S3D' and S3G); however, as this difference still fell within the wild-type R8 subtype proportion, we conclude that the

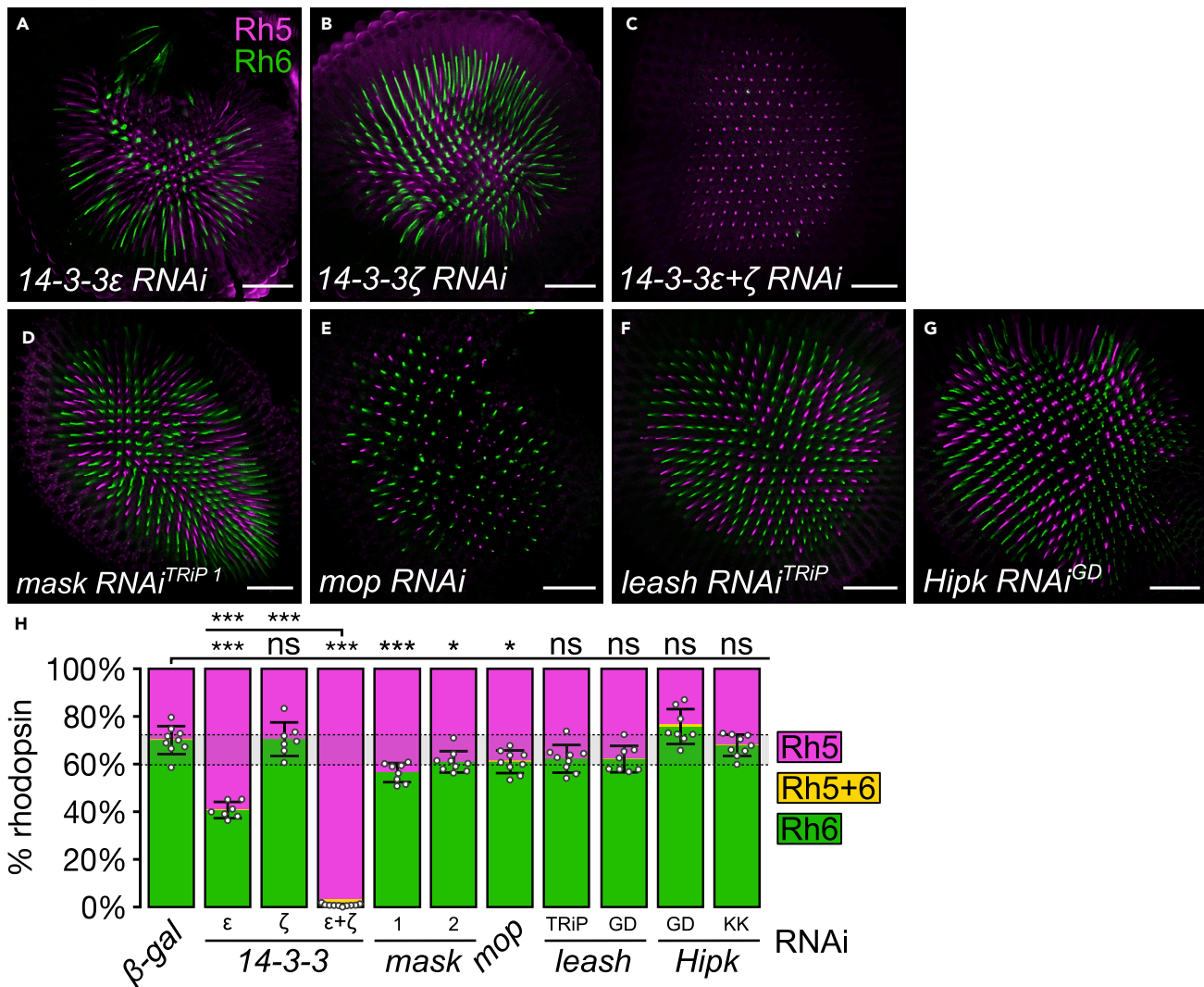


**Figure 4. The 14-3-3 proteins, Mask, and Myopic promote yR8 cell fate**

(A–G) Confocal microscope images of adult *Drosophila* retinas stained with anti-Rh5 (magenta) and anti-Rh6 (green) antibodies. All lines were driven by *IGMR-Gal4*. Retinas expressed *14-3-3 $\epsilon$  RNAi* (A), *14-3-3 $\zeta$  RNAi* (B), both *14-3-3 $\epsilon$  RNAi* and *14-3-3 $\zeta$  RNAi* (C), *mask RNAi<sup>TRiP JF01147</sup>* (D), *mop RNAi* (E), *leash RNAi<sup>TRiP</sup>* (F), and *Hipk RNAi<sup>GD</sup>* (G). Scale bars are 50  $\mu$ m.

(H) Proportion of R8 cells that express Rh5 (magenta), Rh6 (green), or both (yellow). The error bars represent the standard deviation of total % Rh5 (% Rh5 + % Rh5+Rh6). Total % Rh5 was compared with two-sided, unpaired t test; ns, not significant, \*p < 0.01, \*\*\*p < 0.0001. The shaded gray region between the dotted gray lines indicates wild-type Rh5:Rh6 ratio range. Error bars are  $\pm$  SD.  $\beta$ -gal RNAi (Figure 1D): n = 9 retinas, 3,976 ommatidia; *14-3-3 $\epsilon$  RNAi*: n = 7, 1,886; *14-3-3 $\zeta$  RNAi*: n = 7, 1,977; *14-3-3 $\epsilon$ + $\zeta$  RNAi*: n = 10, 1,699; *mask RNAi<sup>TRiP 1</sup>*: n = 8, 2,229; *mask RNAi<sup>TRiP 2</sup>*: n = 9, 3,915; *mop RNAi*: n = 9, 1,767; *leash RNAi<sup>TRiP</sup>*: n = 9, 2,834; *leash RNAi<sup>GD</sup>*: n = 8, 1,734; *Hipk RNAi<sup>GD</sup>*: n = 8, 2,495; *HipK RNAi<sup>KK</sup>*: n = 9, 2,133. See also Figure S1.

addition of the Venus tag has minimal effect on Wts function. Previous studies found that *wts* is only expressed in yR8 cells and not in pR8 cells, as determined by the expression of *wts-LacZ* and *wts-Gal4* (Jukam and Desplan, 2011; Mikeladze-Dvali et al., 2005). Consistent with this, *Wts-Venus* was largely absent from adult pR8 cells but present weakly in the cytoplasm of yR8 cells (Figure 5A). In pupal eyes at 70 h after puparium formation (APF), immediately before Rh5 and Rh6 expression ensues, *Wts-Venus* was detectable in all R8 cells but expressed at higher levels in select cells, which we predict to be the presumptive yR8 cells but are yet to express *Rhodopsin 6* (Figure 5B). By contrast, all other Hippo pathway proteins that we examined were expressed equivalently in both pR8 and yR8 cells (Figures 6A–6H).

In addition, we observed that most Hippo pathway proteins were expressed at dramatically lower levels in pupal and adult eyes than in larval eye imaginal discs. To quantify this, we recombined our endogenously

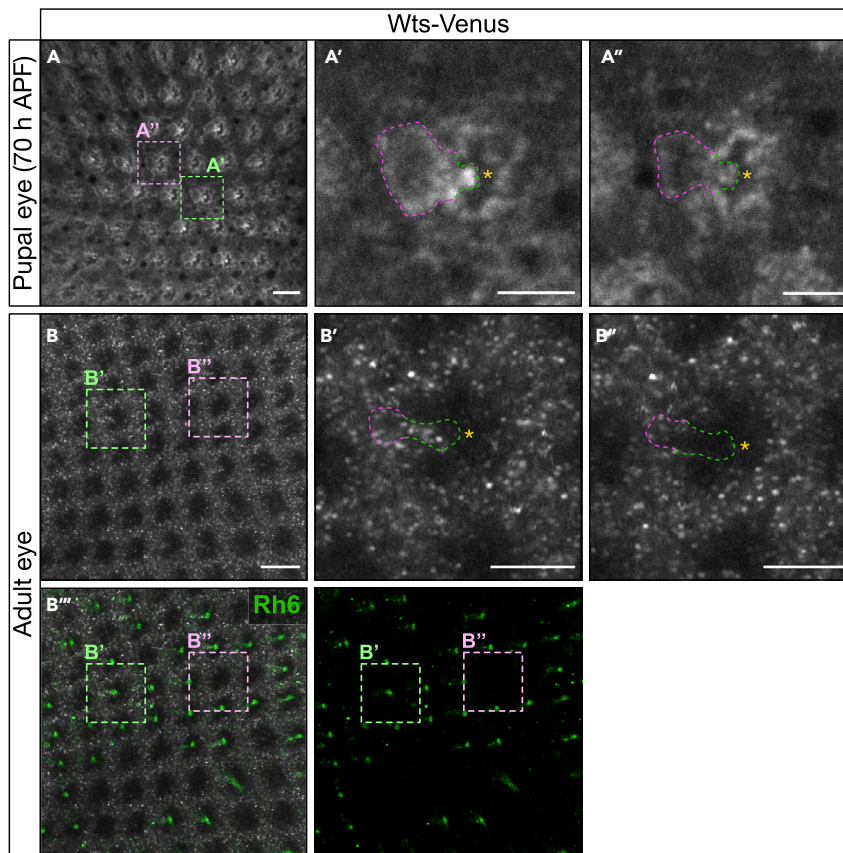


**Figure 5. Warts protein levels are higher in yR8 cells than in pR8 cells**

(A–B'') Confocal microscope images of adult and late pupal (70 h after puparium formation, APF) *Drosophila* retinas. Endogenously tagged Wts-Venus was stained with an anti-GFP antibody to amplify the Venus signal, and anti-Rh6 antibody (green) in adult eyes to show yR8 cells. In each image, anterior is to the left. The dashed boxes in A, A'' and B indicate the area shown in A'-A'' and B'-B'', respectively. A' and B' show high-Wts cells; A'' and B'' show low-Wts cells. Yellow asterisks indicate the R8 rhabdomere. R8 cell outlines are shown by the dashed lines; the green line outlines the apical domain of the cell and the magenta line outlines the basal domain of the cell. Scale bars are 10  $\mu$ m in A and B and 5  $\mu$ m in A'-A'' and B'-B''. See also [Figures S3](#) and [S4](#).

tagged strains onto FRT chromosomes. This allowed us to generate clones of Wts-Venus, Hpo-Venus, and Kibra-Venus using the *eyeless* promoter and compare these to neighboring Venus-negative clones, which served as internal reference points for expression. In Wts-Venus, Hpo-Venus, and Kibra-Venus mosaic tissues, the Venus-tagged proteins were expressed at substantially higher levels in larval eyes than in pupal or adult eyes ( $p < 0.0001$ ) ([Figure 7](#)).

### The subcellular localization of Merlin and Tao in R8 cells changes during late pupal eye development

In larval imaginal discs, Hippo pathway activity is regulated by partitioning of different proteins to specialized membrane subdomains ([Su et al., 2017](#); [Sun et al., 2015](#)). To determine whether this feature of Hippo signaling is also important in R8 cells, we examined the localization of Hippo pathway proteins at two stages of development—pupal eyes (70 h APF), when R8 cell fate is being specified by the Hippo pathway, and adult eyes, when the Hippo pathway is important for maintaining R8 cell fate ([Jukam and Desplan, 2011](#)). Interestingly, we found that Wts, Hpo, and Kibra did not obviously localize to specific membrane domains and instead were present throughout the cytoplasm of both pupal and adult R8 cells ([Figures 5A–5B''](#), [6E–6H'](#), and [S4A–S4H](#)). However, higher-resolution imaging approaches such as electron microscopy are likely to be required to definitively conclude whether these proteins are only present in the cytoplasm of R8 cells or whether they also reside on specific cellular membranes. By contrast, Mer and Tao were both

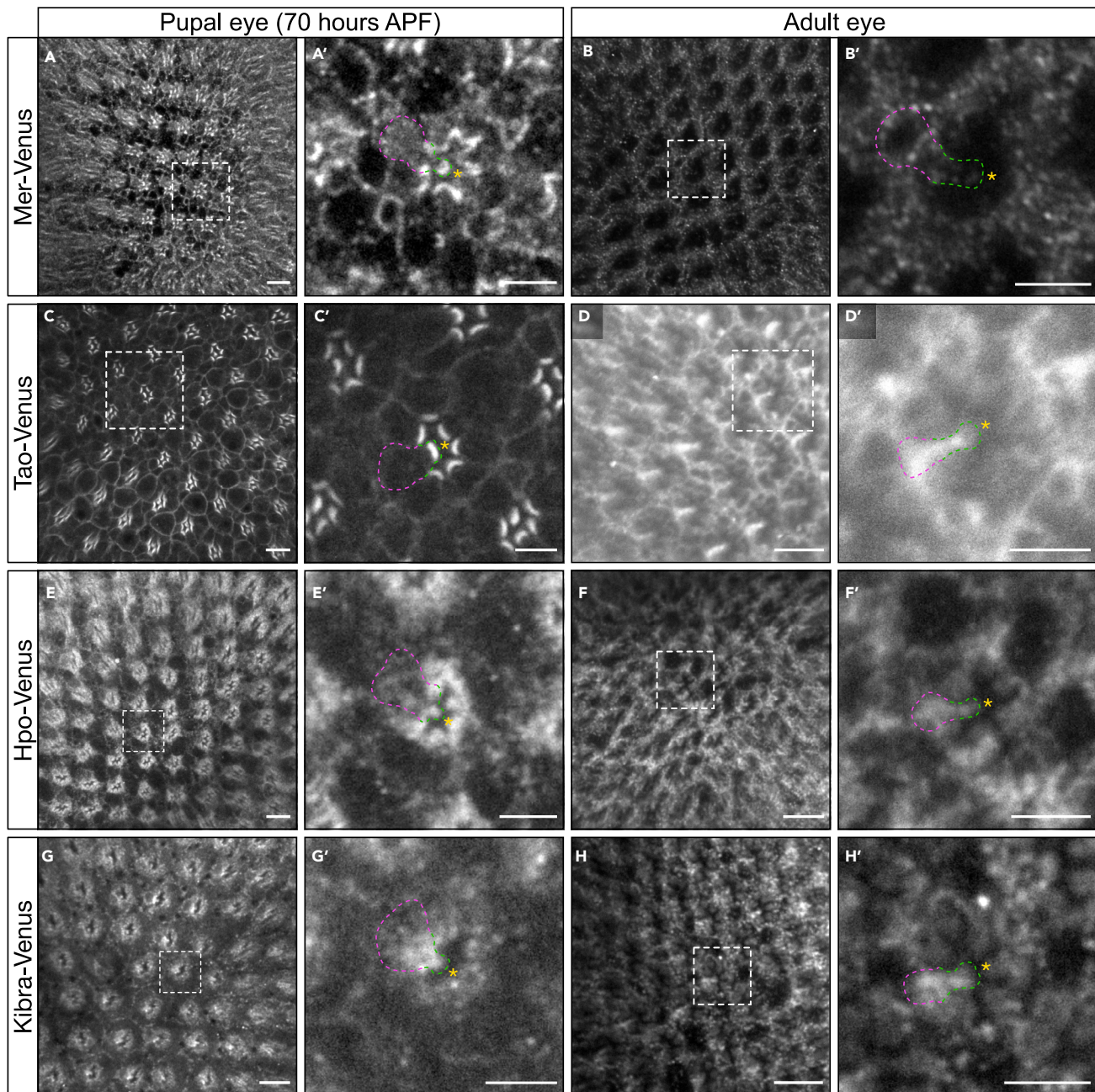


**Figure 6. Subcellular localization of Merlin and Tao differ in late pupal and adult R8 cells**

(A–H') Confocal microscope images of late pupal (70 h APF) and adult *Drosophila* retinas. Endogenously tagged Mer-Venus (A–B'), Tao-Venus (C–D'), Hpo-Venus (E–F'), and Kibra-Venus (G–H') retinas were stained with an anti-GFP antibody to amplify the Venus signal. In each image, anterior is to the left. The dashed white boxes in A–F indicate the area shown in A'–F', respectively. Yellow asterisks indicate the R8 rhabdome. R8 cell outlines are shown by the dashed lines; the green line outlines the apical domain of the cell and the magenta line outlines the basal domain of the cell. Scale bars are 10  $\mu\text{m}$  in A–F and 5  $\mu\text{m}$  in A'–F'. See also Figures S3–S5.

enriched apically and, furthermore, their localization differed drastically between late pupal and adult R8 cells (Figures 6A–6D' and S4I–S4L). At 70 h APF, Mer-Venus and Tao-Venus both localized strongly at the rhabdome, while Mer-Venus also localized at adherens junctions (Figures 6A–6A', 6C–6C', S4J, and S4L). In adult R8 cells, however, both Mer-Venus and Tao-Venus localized at the stalk membrane, between the rhabdome and the adherens junctions (Figures 6B, 6B', 6D, 6D', S4I, and S4K). The timing of these changes in subcellular localization of Mer, Tao was also observed for  $\alpha$ -Spectrin ( $\alpha$ -Spec), which we

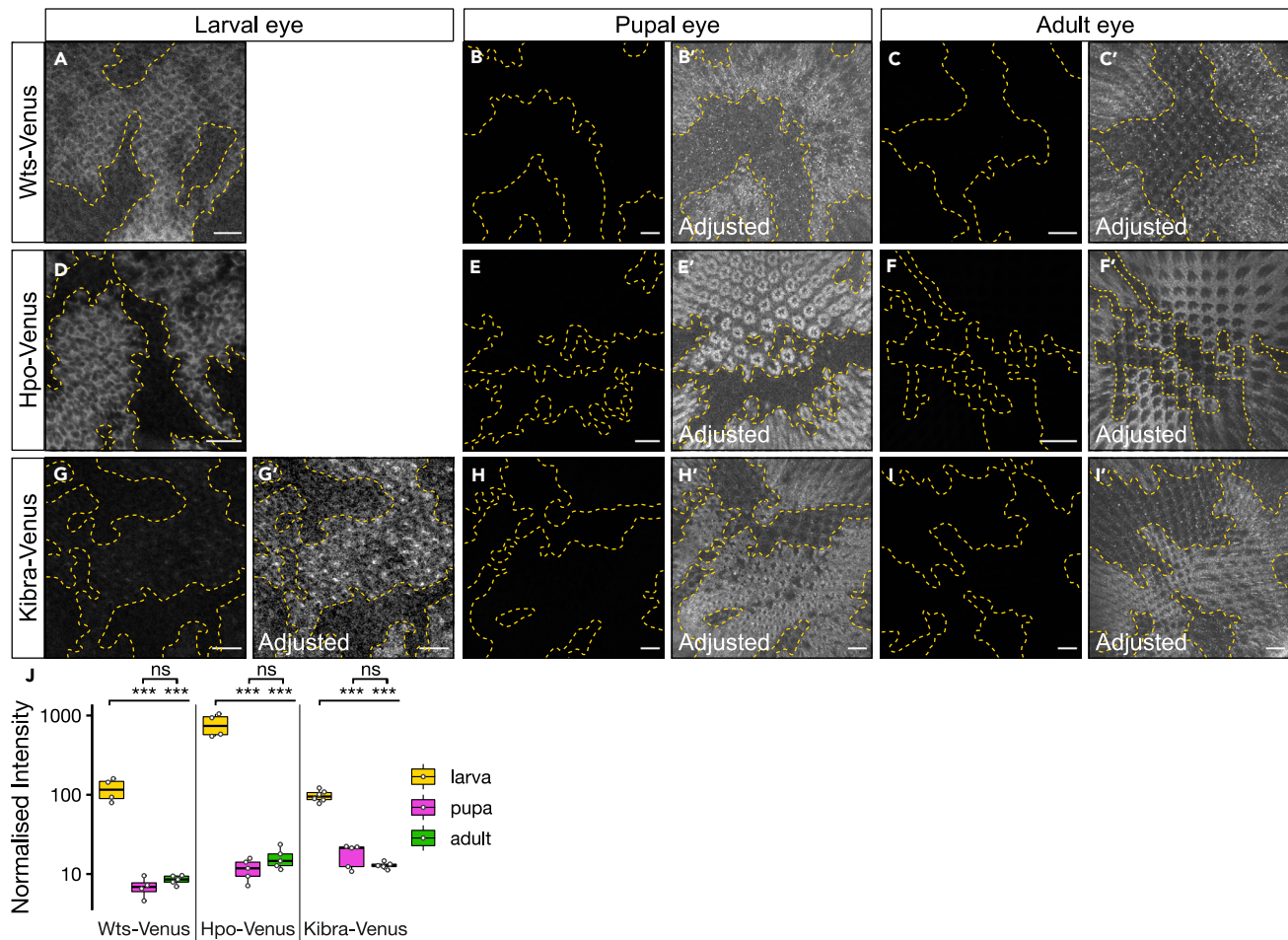


**Figure 7. Hippo pathway proteins are expressed at lower levels in pupal and adult eyes than in larval eyes**

(A–I') Confocal microscope images of larval eye imaginal discs (A, D, G–G'), late pupal (70 h APF) retinas (B–B', E–E', and H–H'), and adult retinas (C–C', F–F', and I–I'). Clones of endogenously tagged Wts-Venus (A–C'), Hpo-Venus (D–F'), and Kibra-Venus (G–I') retinas were stained with an anti-GFP antibody to amplify the Venus signal. Yellow outlines show clonal boundaries. Tissues for each genotype were imaged with identical laser intensity. B', C', E', F', G', H', and I' have increased contrast to visualize clonal tissue that cannot be seen in B, C, E, F, G, H, and I, respectively. Scale bars are 20  $\mu$ m.

(J) Quantification of Venus intensity in Venus-expressing clones, normalized to background autofluorescence in Venus-negative clones. Tissues were compared with an ANOVA and Tukey's HSD Test; ns, not significant; \*\*\* $p$  < 0.001.

reported recently as a protein that can influence R8 cell fate (Pojer et al., 2021). Next, we investigated this with greater temporal resolution and found that Mer, Tao, and  $\alpha$ -Spec all underwent their dramatic changes in subcellular localization in a 6-h window, between 88 and 94 h APF (Figure S5), suggesting a potential functional link between these proteins in R8 cells.

## DISCUSSION

Like many signaling pathways, the Hippo pathway is deployed to perform multiple functions. For example, it regulates the growth of the *D. melanogaster* eye during development and then controls R8 cell fate choice in the post-mitotic pupal and adult eye. To date, Hippo signal transduction has been predominantly characterized in the context of organ growth, as opposed to R8 cell fate. To redress this deficiency, we studied Hippo signaling in R8 cells and identified a further eight Hippo pathway proteins that play some role in R8 cell fate control (Figure 8A). The core STRIPAK components, Cka and Mts; Tao; Pez; the 14-3-3 proteins; Mask; and Mop all influence the binary cell fate decision of R8 photoreceptor cells, whereas other proteins that influence Hippo-dependent organ growth, including Slmap, Hipk, and Leash, do not obviously regulate R8 cell fate. This provides new insights into R8 cell fate specification and highlights variations in Hippo signaling in different biological settings.

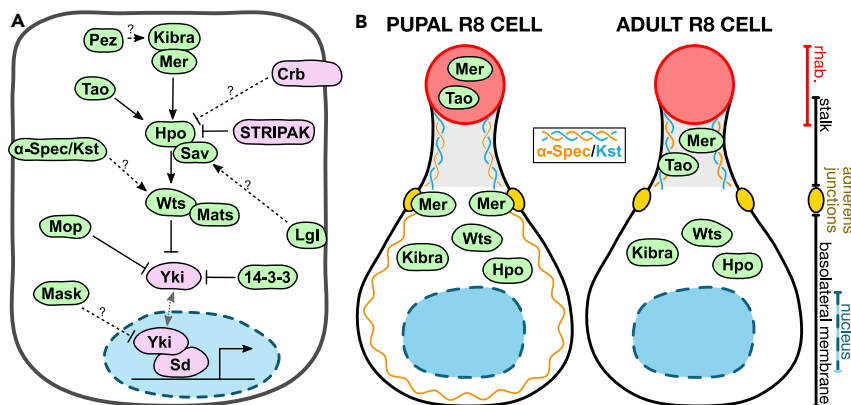


**Figure 8. Model of the Hippo pathway in R8 cells**

(A) Schematic diagram of the Hippo pathway in R8 cells. Proteins labeled in magenta promote pR8 cell fate, whereas proteins labeled in green promote yR8 cell fate.  $\alpha$ -Spec,  $\alpha$ -Spectrin; Crb, Crumbs; Hpo, Hippo; Kst, Karst; Lgl, Lethal (2) giant larvae; Mats, Mob as tumor suppressor; Mer, Merlin; Mop, Myopic; Sav, Salvador; Sd, Scalloped; STRIPAK, Striatin-interacting phosphatase and kinase; Wts, Warts; Yki, Yorkie.

(B) Schematic diagrams of the pupal and adult R8 cell, showing localization of Wts, Hpo, Kibra, Mer, Tao,  $\alpha$ -Spec, and Kst in each stage of development. The rhabdome (rhab.; red), adherens junctions (yellow), and the nucleus (blue) are indicated.

A surprising result was that, although the core STRIPAK components, Cka and Mts, promote pR8 cell fate, consistent with their roles as negative regulators of Hpo (Ribeiro et al., 2010), the adaptor proteins, Slmap and Rassf, do not obviously regulate R8 cell fate (Jukam and Desplan, 2011). This raises the possibility that an additional adaptor protein links the STRIPAK complex to Hpo in R8 cells. In growing organs and neural stem cells, Tao acts in opposition to STRIPAK by phosphorylating the Hpo activation loop motif and activating it (Boggiano et al., 2011; Poon et al., 2011, 2016). Our study indicates that opposing regulation of Hpo by Tao and STRIPAK is also important for R8 cell fate specification.

In R8 cells, several important regulatory steps impinge directly on Yki, with the best described of these being the bistable feedback loop that includes Wts and Melt (Jukam et al., 2013). Here, we identified four proteins that have been shown to form a physical complex with Yki that also influence R8 cell fate—the two 14-3-3 proteins, Mop, and Mask—all of which promote yR8 cell fate. The role of the 14-3-3 proteins in R8 cells is consistent with their role in growing organs where they promote the cytoplasmic pool of Yki in response to Wts phosphorylation (Ren et al., 2010). Our study also suggests a minor role for Mop in Yki suppression, consistent with a prior study in imaginal disc growth (Gilbert et al., 2011). Mask is a Yki cofactor that promotes expression of Yki-dependent genes in epithelial tissue growth (Sansores-Garcia et al., 2013; Sidor et al., 2013). Surprisingly, we found that Mask promotes yR8 cell fate, i.e., RNAi-mediated depletion of Mask caused an increase in pR8 fate, which is normally driven by Yki. The reason for the seemingly opposing actions of Mask on Yki activity in growing imaginal discs and R8 cell fate is unclear and requires further investigation.

In growing larval imaginal discs, a key feature of control of Hippo pathway activity is the localization of pathway proteins to specialized membrane domains (Su et al., 2017; Sun et al., 2015). The mechano-sensitive proteins  $\alpha$ -catenin and Jub recruit Wts to adherens junctions and hold it in an inactive state (Rauskolb et al., 2014; Sun et al., 2015). Multiple Hippo pathway proteins including Ex, Mer, Kibra, Hpo, and Sav also co-localize with Wts at the sub-apical region and medial apical cortex of imaginal disc cells, where Wts is thought to be activated (Su et al., 2017; Sun et al., 2015). By contrast, in R8 cells, we found that most Hippo pathway proteins were predominantly cytoplasmic rather than enriched at particular membrane domains (Figure 8B). In addition, Jub expression was undetectable in adult eyes and does not influence R8 cell fate (Pojer et al., 2021). This suggests that Wts regulation by Jub and mechanical forces do not operate in R8 cells and also explains why Wts is not detected at adherens junctions of R8 cells. Instead, the cytoplasm appears to be the major site of Hippo pathway activation in R8 cells, although we cannot rule out the possibility that specific membrane domains are also important and that Hippo pathway proteins only localize there transiently in order to be regulated. Furthermore, Mer and Tao localized primarily to the rhabdome

of pupal R8 cells but in the cytoplasm of adult R8 cells (Figure 8B), suggesting that the subcellular compartment where the Hippo pathway is regulated in R8 cells could differ throughout eye development.

By surveying the expression of select Hippo pathway proteins in pupal and adult eyes, we found Wts to be the only protein to be differentially expressed between R8 subtypes (i.e., it is expressed more strongly in yR8 cells than in pR8 cells). This is consistent with the observation that Yki, Sd, and Melt regulate *wts* transcription in R8 cells, resulting in suppression of its expression in the pR8 subtype (Jukam et al., 2013; Mike-ladze-Dvali et al., 2005). In contrast, Hippo pathway proteins that operate upstream of Wts did not obviously differ either in expression or subcellular localization between R8 subtypes. Together, these results suggest that regulation of both Wts activity and *wts* transcription are important for R8 cell fate. In yR8 cells, *wts* is expressed and Wts is activated by upstream Hippo pathway proteins to regulate R8 cell fate. In pR8 cells, however, Yki and Sd regulate cell fate through a feedforward loop that results in the repression of *wts* transcription (Jukam et al., 2013). Our results show that upstream Hippo pathway components are also expressed in pR8 cells but presumably cannot repress Yki in the absence of Wts. This suggests that the key difference in the Hippo pathway between pR8 and yR8 cells is the expression level of *wts*, rather than Hippo pathway activity being dictated by upstream pathway proteins and/or an external signal, and that the Hippo pathway is competent to activate Wts in all R8 cells. This notion is reinforced by the observation that R8 cell fate can be modulated simply by altering the expression of different Hippo pathway proteins (Jukam and Desplan, 2011), indicating that the signal transduction capacity of the Hippo pathway is intact in naive R8 cells.

Interestingly, the key Hippo pathway proteins Wts, Hpo, and Kibra were all expressed at substantially lower levels in the post-mitotic eye (pupal and adult stages) than in the actively growing larval eye, which is consistent with earlier studies that found that Ex is similarly downregulated in the post-mitotic eye (Milton et al., 2010). One possibility is that core Hippo pathway proteins need to be expressed at low levels in the pupal and adult eye so that only minor fluctuations in Wts abundance in pupal R8 cells can lead to changes in cell fate that are elicited by differential Yki activity. In any case, it is interesting that, upon the cessation of organ growth, the expression of many central Hippo pathway proteins is downregulated, as opposed to only those genes that promote organ growth. Broadly, this resembles observations in T cell development, where key Hippo pathway genes (e.g., Yap, Lats1, Mob1, Sav1, Tead1, and Tead3) are largely absent from naive murine T cells but are expressed in late-stage CD8+ T cells (Thaventhiran et al., 2012). In both situations, fluctuations in the abundance of both positive and negative regulators of Hippo pathway are correlated. Presumably this facilitates changes in the magnitude of Yki/Yap activity but still allows Yki/Yap activity to be tightly controlled by the Hippo pathway. It also probably reflects the fact that the expression of many upstream Hippo pathway genes is regulated by Yki/YAP in negative feedback loops.

Our studies highlight important similarities and differences between Hippo signaling in organ growth control and R8 photoreceptor cell fate choice. Similar to other instances where the Hippo pathway is integral for cell fate specification, such as the posterior follicle cells of the *D. melanogaster* ovary (Meignin et al., 2007; Polesello and Tapon, 2007; Yu et al., 2008), only subsets of Hippo pathway growth regulatory proteins are required for correct R8 cell fate choice. Furthermore, the importance of subcellular localization of Hippo pathway proteins for their regulation appears to vary in different developmental contexts and cell types.

### Limitations of the study

- Developing eye tissues grow poorly when harboring mutant alleles of Hippo pathway genes that normally promote tissue growth. As such, restricted expression of RNAi lines was used instead of mutant alleles to assess the role of such Hippo pathway genes in R8 cell fate.
- Many proteins examined in this paper are expressed at low levels within R8 cells, making protein subcellular localization difficult to determine.

### STAR★METHODS

Detailed methods are provided in the online version of this paper and include the following:

- KEY RESOURCES TABLE
- RESOURCE AVAILABILITY
  - Lead contact

- Materials availability
- Data and code availability
- EXPERIMENTAL MODEL AND SUBJECT DETAILS
- METHOD DETAILS
- QUANTIFICATION AND STATISTICAL ANALYSIS

## SUPPLEMENTAL INFORMATION

Supplemental information can be found online at <https://doi.org/10.1016/j.isci.2021.102830>.

## ACKNOWLEDGMENTS

We thank C. Desplan for comments on the manuscript and reagents and R. Johnston, the Bloomington *Drosophila* Stock Center, the Vienna *Drosophila* RNAi Center, the Australian *Drosophila* Research Support Facility ([www.ozdros.com](http://www.ozdros.com)), and the Developmental Studies Hybridoma Bank for *D. melanogaster* stocks and antibodies. K.F.H. was supported by a Senior Research Fellowship (APP1078220) and Investigator grant (APP1194467) from the National Health and Medical Research Council (NHMRC) and J.M.P. was supported by an Australian Postgraduate Award. This research was supported by the Australian Research Council (DP180102044) and the NHMRC (APP1157737). We acknowledge the Peter Mac Centre for Advanced Histology and Microscopy and support to them from the Peter MacCallum Cancer Foundation and the Australian Cancer Research Foundation.

## AUTHOR CONTRIBUTIONS

Conceptualization, J.M.P. and K.F.H.; methodology, J.M.P. and K.F.H.; validation, J.M.P., S.A.M., and B.K.; investigation, J.M.P. and S.A.M.; resources: S.K.; writing – original draft, J.M.P. and K.F.H.; writing – review & editing, J.M.P. and K.F.H.; visualization, J.M.P.; supervision, K.F.H.; funding acquisition, K.F.H.

## DECLARATION OF INTERESTS

The authors declare no competing interests.

Received: October 30, 2020

Revised: June 1, 2021

Accepted: July 7, 2021

Published: August 20, 2021

## REFERENCES

- Acevedo, S.F., Tsigkari, K.K., Grammenoudi, S., and Skoulakis, E.M.C. (2007). In vivo functional specificity and homeostasis of *Drosophila* 14-3-3 proteins. *Genetics* 177, 239–253. <https://doi.org/10.1534/genetics.107.072280>.
- Baumgartner, R., Poernbacher, I., Buser, N., Hafen, E., and Stocker, H. (2010). The WW domain protein Kibra acts upstream of hippo in *Drosophila*. *Dev. Cell* 18, 309–316. <https://doi.org/10.1016/j.devcel.2009.12.013>.
- Boggiano, J.C., Vanderzalm, P.J., and Fehon, R.G. (2011). Tao-1 phosphorylates Hippo/MST kinases to regulate the Hippo-Salvador-Warts tumor suppressor pathway. *Dev. Cell* 21, 888–895. <https://doi.org/10.1016/j.devcel.2011.08.028>.
- Chen, J., and Verheyen, E.M. (2012). Homeodomain-interacting protein kinase regulates yorkie activity to promote tissue growth. *Curr. Biol.* 22, 1582–1586. <https://doi.org/10.1016/j.cub.2012.06.074>.
- Clarke, E., and Sherrill-Mix, S. (2017). Ggbeeswarm: Categorical Scatter (Violin Point) Plots.
- Gaspar, P., and Tapon, N. (2014). Sensing the local environment: actin architecture and Hippo signalling. *Curr. Opin. Cell Biol.* 31, 74–83. <https://doi.org/10.1016/j.cob.2014.09.003>.
- Genevet, A., Wehr, M.C., Brain, R., Thompson, B.J., and Tapon, N. (2010). Kibra is a regulator of the salvador/warts/hippo signaling network. *Dev. Cell* 18, 300–308. <https://doi.org/10.1016/j.devcel.2009.12.011>.
- Gilbert, M.M., Tipping, M., Veraksa, A., and Moberg, K.H. (2011). A screen for conditional growth suppressor genes identifies the *Drosophila* homolog of HD-PTP as a regulator of the oncoprotein yorkie. *Dev. Cell* 20, 700–712. <https://doi.org/10.1016/j.devcel.2011.04.012>.
- Goulev, Y., Fauny, J.D., Gonzalez-Marti, B., Flagiello, D., Silber, J., and Zider, A. (2008). SCALLOPED interacts with YORKIE, the nuclear effector of the hippo tumor-suppressor pathway in *Drosophila*. *Curr. Biol.* 18, 435–441. <https://doi.org/10.1016/j.cub.2008.02.034>.
- Hamaratoglu, F., Willecke, M., Kango-Singh, M., Nolo, R., Hyun, E., Tao, C., Jafar-Nejad, H., and Halder, G. (2006). The tumour-suppressor genes NF2/Merlin and Expanded act through Hippo signalling to regulate cell proliferation and apoptosis. *Nat. Cell Biol.* 8, 27–36. <https://doi.org/10.1038/ncb1339>.
- Harvey, K.F., Pflieger, C.M., and Hariharan, I.K. (2003). The *Drosophila* Mst ortholog, hippo, restricts growth and cell proliferation and promotes apoptosis. *Cell* 114, 457–467.
- Harvey, K.F., Zhang, X., and Thomas, D.M. (2013). The Hippo pathway and human cancer. *Nat. Rev. Cancer* 13, 246–257. <https://doi.org/10.1038/nrc3458>.
- Hsiao, H.-Y., Johnston, R.J., Jukam, D., Vasiliauskas, D., Desplan, C., and Rister, J. (2012). Dissection and immunohistochemistry of larval, pupal and adult *Drosophila* retinas. *J. Vis. Exp.* 69, e4347. <https://doi.org/10.3791/4347>.
- Irvine, K.D., and Harvey, K.F. (2015). Control of organ growth by patterning and hippo signaling in *drosophila*. *Cold Spring Harb. Perspect. Biol.* 7, 1–16. <https://doi.org/10.1101/cshperspect.a019224>.
- Jia, J., Zhang, W., Wang, B., Trinko, R., and Jiang, J. (2003). The *Drosophila* Ste20 family kinase dMST functions as a tumor suppressor by

restricting cell proliferation and promoting apoptosis. *Genes Dev.* 17, 2514–2519. <https://doi.org/10.1101/gad.1134003>.

Johnston, R.J., and Desplan, C. (2014). Interchromosomal communication coordinates intrinsically stochastic expression between alleles. *Science* 343, 661–665. <https://doi.org/10.1038/nn.2877>.

Jukam, D., and Desplan, C. (2011). Binary regulation of Hippo pathway by Merlin/NF2, Kibra, Lgl, and melted specifies and maintains postmitotic neuronal fate. *Dev. Cell* 21, 874–887. <https://doi.org/10.1016/j.devcel.2011.10.004>.

Jukam, D., Xie, B., Rister, J., Terrell, D., Charlton-Perkins, M.A., Pistillo, D., Gebelein, B., Desplan, C., and Cook, T. (2013). Opposite feedbacks in the Hippo pathway for growth control and neural fate. *Science* 342, 1238016. <https://doi.org/10.1126/science.1238016>.

Justice, R.W., Zilian, O., Woods, D.F., Noll, M., and Bryant, P.J. (1995). The *Drosophila* tumor-suppressor gene *warts* encodes a homolog of human myotonic-dystrophy kinase and is required for the control of cell-shape and proliferation. *Genes Dev.* 9, 534–546. <https://doi.org/10.1101/Gad.9.5.534>.

Kango-Singh, M., Nolo, R., Tao, C., Verstreken, P., Hiesinger, P.R., Bellen, H.J., and Halder, G. (2002). *Shar-pei* mediates cell proliferation arrest during imaginal disc growth in *Drosophila*. *Development* 129, 5719–5730. <https://doi.org/10.1242/dev.00168>.

Kulkarni, A., Chang, M.T., Vissers, J.H.A., Dey, A., and Harvey, K.F. (2020). The hippo pathway as a driver of select human cancers. *Trends Cancer* 6, 781–796. <https://doi.org/10.1016/j.trecan.2020.04.004>.

Kwon, Y., Vinayagam, A., Sun, X., Dephoure, N., Gygi, S.P., Hong, P., and Perrimon, N. (2013). The hippo signaling pathway interactome. *Science* 342, 737–741.

Lai, Z.-C., Wei, X., Shimizu, T., Ramos, E., Rohrbach, M., Nikolaidis, N., Ho, L.-L., and Li, Y. (2005). Control of cell proliferation and apoptosis by *mob* as tumor suppressor. *Cell* 120, 675–685. <https://doi.org/10.1016/j.cell.2004.12.036>.

Meignin, C., Alvarez-Garcia, I., Davis, I., and Palacios, I.M. (2007). The salvador-warts-hippo pathway is required for epithelial proliferation and Axis specification in *Drosophila*. *Curr. Biol.* 17, 1871–1878. <https://doi.org/10.1016/j.cub.2007.09.062>.

Mikeladze-Dvali, T., Wernet, M.F., Pistillo, D., Mazzoni, E.O., Teleman, A.A., Chen, Y.W., Cohen, S.M., and Desplan, C. (2005). The growth regulators *warts/lats* and *melted* interact in a bistable loop to specify opposite fates in *Drosophila* R8 photoreceptors. *Cell* 122, 775–787. <https://doi.org/10.1016/j.cell.2005.07.026>.

Milton, C.C., Zhang, X., Albanese, N.O., and Harvey, K.F. (2010). Differential requirement of Salvador-Warts-Hippo pathway members for organ size control in *Drosophila melanogaster*. *Development* 137, 735–743. <https://doi.org/10.1242/dev.042309>.

Morante, J., and Desplan, C. (2011). Protocol dissection and staining of *Drosophila* optic lobes at different stages of development. *Cold Spring Harb. Protoc.* 6, 652–657. <https://doi.org/10.1101/pdb.prot5629>.

Pantalacci, S., Tapon, N., and Léopold, P. (2003). The Salvador partner Hippo promotes apoptosis and cell-cycle exit in *Drosophila*. *Nat. Cell Biol.* 5, 921–927. <https://doi.org/10.1038/ncb1051>.

Poernbacher, I., Baumgartner, R., Marada, S.K., Edwards, K., and Stocker, H. (2012). *Drosophila* *Pez* acts in hippo signaling to restrict intestinal stem cell proliferation. *Curr. Biol.* 22, 389–396. <https://doi.org/10.1016/j.cub.2012.01.019>.

Pojer, J.M., Saiful Hilmi, A.J., Kondo, S., and Harvey, K.F. (2021). Crumbs and the apical spectrin cytoskeleton regulate R8 cell fate in the *Drosophila* eye. *Plos Genet.* 17, e1009146. <https://doi.org/10.1371/journal.pgen.1009146>.

Polesello, C., and Tapon, N. (2007). Salvador-Warts-Hippo signaling promotes *Drosophila* posterior follicle cell maturation downstream of notch. *Curr. Biol.* 17, 1864–1870. <https://doi.org/10.1016/j.cub.2007.09.049>.

Poon, C.L.C., Lin, J.I., Zhang, X., and Harvey, K.F. (2011). The sterile 20-like kinase *Tao-1* controls tissue growth by regulating the Salvador-Warts-Hippo pathway. *Dev. Cell* 21, 896–906. <https://doi.org/10.1016/j.devcel.2011.09.012>.

Poon, C.L.C., Liu, W., Song, Y., Gomez, M., Kulaberoglu, Y., Zhang, X., Xu, W., Veraksa, A., Hergovich, A., Ghabrial, A., et al. (2018). A hippo-like signaling pathway controls tracheal morphogenesis in *Drosophila melanogaster*. *Dev. Cell* 47, 564–575. <https://doi.org/10.1016/j.devcel.2018.09.024>.

Poon, C.L.C., Mitchell, K.A., Kondo, S., Cheng, L.Y., and Harvey, K.F. (2016). The hippo pathway regulates neuroblasts and brain size in *Drosophila melanogaster*. *Curr. Biol.* 26, 1034–1042. <https://doi.org/10.1016/j.cub.2016.02.009>.

Poon, C.L.C., Zhang, X., Lin, J.I., Manning, S.A., and Harvey, K.F. (2012). Homeodomain-interacting protein kinase regulates Hippo pathway-dependent tissue growth. *Curr. Biol.* 22, 1587–1594. <https://doi.org/10.1016/j.cub.2012.06.075>.

Rauskolb, C., Sun, S., Sun, G., Pan, Y., and Irvine, K.D. (2014). Cytoskeletal tension inhibits Hippo signaling through an Ajuba-Warts complex. *Cell* 158, 143–156. <https://doi.org/10.1016/j.cell.2014.05.035>.

Ready, D.F. (2002). *Drosophila* compound eye morphogenesis: blind mechanical engineers? In *Results and Problems in Cell Differentiation: Drosophila Eye Development*, 37, E. Moses, ed (Springer-Verlag), pp. 191–204.

Ren, F., Zhang, L., and Jiang, J. (2010). Hippo signaling regulates Yorkie nuclear localization and activity through 14-3-3 dependent and independent mechanisms. *Dev. Biol.* 337, 303–312. <https://doi.org/10.1016/j.ydbio.2009.10.046>.

Ribeiro, P.S., Josue, F., Wepf, A., Wehr, M.C., Rinner, O., Kelly, G., Tapon, N., and Gsaiger, M. (2010). Combined functional genomic and proteomic approaches identify a PP2A complex

as a negative regulator of hippo signaling. *Mol. Cell* 39, 521–534. <https://doi.org/10.1016/j.molcel.2010.08.002>.

RStudio Team (2020). RStudio (Integrated Development for R. RStudio, PBC).

Sansores-Garcia, L., Atkins, M., Moya, I.M., Shahmoradgoli, M., Tao, C., Mills, G.B., and Halder, G. (2013). Mask is required for the activity of the hippo pathway effector *yki/YAP*. *Curr. Biol.* 23, 229–235. <https://doi.org/10.1016/j.cub.2012.12.033>.

Schindelin, J., Arganda-Carreras, I., Frise, E., Kaynig, V., Longair, M., Pietzsch, T., Preibisch, S., Rueden, C., Saalfeld, S., Schmid, B., et al. (2012). Fiji: an open-source platform for biological-image analysis. *Nat. Methods* 9, 676–682. <https://doi.org/10.1038/nmeth.2019>.

Schnaitmann, C., Garbers, C., Wachtler, T., and Tanimoto, H. (2013). Color discrimination with broadband photoreceptors. *Curr. Biol.* 23, 2375–2382. <https://doi.org/10.1016/j.cub.2013.10.037>.

Schroeder, M.C., and Halder, G. (2012). Regulation of the Hippo pathway by cell architecture and mechanical signals. *Semin. Cell Dev. Biol.* 23, 803–811. <https://doi.org/10.1016/j.semcdb.2012.06.001>.

Sharkey, C.R., Blanco, J., Leibowitz, M.M., Pinto-Benito, D., and Wardill, T.J. (2020). The spectral sensitivity of *Drosophila* photoreceptors. *bioRxiv*, 2020.04.03.024638.

Sidor, C.M., Brain, R., and Thompson, B.J. (2013). Mask proteins are cofactors of *yorkie/YAP* in the hippo pathway. *Curr. Biol.* 23, 223–228. <https://doi.org/10.1016/j.cub.2012.11.061>.

Su, T., Ludwig, M.Z., Xu, J., and Fehon, R.G. (2017). Kibra and Merlin activate the hippo pathway spatially distinct from and independent of expanded. *Dev. Cell* 40, 478–490. <https://doi.org/10.1016/j.devcel.2017.02.004>.

Sun, S., Reddy, B.V.V.G., and Irvine, K.D. (2015). Localization of Hippo signalling complexes and Warts activation in vivo. *Nat. Commun.* 6, 1–12. <https://doi.org/10.1038/ncomms9402>.

Tapon, N., Harvey, K.F., Bell, D.W., Wahrer, D.C.R., Schiripo, T.A., Haber, D.A., and Hariharan, I.K. (2002). Salvador promotes both cell cycle exit and apoptosis in *Drosophila* and is mutated in human cancer cell lines. *Cell* 110, 467–478. [https://doi.org/10.1016/S0092-8674\(02\)00824-3](https://doi.org/10.1016/S0092-8674(02)00824-3).

Thaventhiran, J.E.D., Hoffmann, A., Magiera, L., De La Roche, M., Lingel, H., Brunner-Weinzierl, M., and Fearon, D.T. (2012). Activation of the Hippo pathway by CTLA-4 regulates the expression of Blimp-1 in the CD8+ T cell. *Proc. Natl. Acad. Sci. U S A* 109, 2223–2229. <https://doi.org/10.1073/pnas.1209115109>.

Udan, R.S., Kango-Singh, M., Nolo, R., Tao, C., and Halder, G. (2003). Hippo promotes proliferation arrest and apoptosis in the Salvador/Warts pathway. *Nat. Cell Biol.* 5, 914–920. <https://doi.org/10.1038/ncb1050>.

Wells, B.S., Pistillo, D., Barnhart, E., and Desplan, C. (2017). Parallel Activin and BMP signaling coordinates R7/R8 photoreceptor subtype pairing in the stochastic *Drosophila* retina. *eLife* 6, e25301.

Wernet, M.F., Labhart, T., Baumann, F., Mazzoni, E.O., Pichaud, F., and Desplan, C. (2003). Homothorax switches function of Drosophila photoreceptors from color to polarized light sensors. *Cell* 115, 267–279. [https://doi.org/10.1016/S0092-8674\(03\)00848-1](https://doi.org/10.1016/S0092-8674(03)00848-1).

Wernet, M.F., Mazzoni, E.O., Celik, A., Duncan, D.M., Duncan, I., and Desplan, C. (2006). Stochastic spineless expression creates the retinal mosaic for colour vision. *Nature* 440, 174–180. <https://doi.org/10.1038/nature04615>.

Wickham, H. (2016). *ggplot2: Elegant Graphics for Data Analysis* (Springer-Verlag).

Wu, S., Huang, J., Dong, J., and Pan, D. (2003). Hippo encodes a Ste-20 family protein kinase that restricts cell proliferation and promotes apoptosis in conjunction with salvador and warts. *Cell* 114, 445–456. [https://doi.org/10.1016/S0092-8674\(03\)00549-X](https://doi.org/10.1016/S0092-8674(03)00549-X).

Wu, S., Liu, Y., Zheng, Y., Dong, J., and Pan, D. (2008). The TEAD/TEF family protein Scalloped mediates transcriptional output of the Hippo

growth-regulatory pathway. *Dev. Cell* 14, 388–398. <https://doi.org/10.1016/j.devcel.2008.01.007>.

Xie, B., Morton, D.B., and Cook, T.A. (2019). Opposing transcriptional and post-transcriptional roles for Scalloped in binary Hippo-dependent neural fate decisions. *Dev. Biol.* 455, 51–59. <https://doi.org/10.1016/j.ydbio.2019.06.022>.

Xu, T., Wang, W., Zhang, S., Stewart, R.A., and Yu, W. (1995). Identifying tumor suppressors in genetic mosaics: the *Drosophila* *lats* gene encodes a putative protein kinase. *Development* 121, 1053–1063.

Yamaguchi, S., Desplan, C., and Heisenberg, M. (2010). Contribution of photoreceptor subtypes to spectral wavelength preference in *Drosophila*. *Proc. Natl. Acad. Sci. U S A* 107, 5634–5639. <https://doi.org/10.1073/pnas.0809398107>.

Yu, J., Poulton, J., Huang, Y.-C., and Deng, W.-M. (2008). The hippo pathway promotes notch

signaling in regulation of cell differentiation, proliferation, and Oocyte polarity. *PLoS One* 3, e1761. <https://doi.org/10.1371/journal.pone.0001761>.

Zhang, L., Ren, F., Zhang, Q., Chen, Y., Wang, B., and Jiang, J. (2008). The TEAD/TEF family of transcription factor Scalloped mediates Hippo signaling in organ size control. *Dev. Cell* 14, 377–387. <https://doi.org/10.1016/j.devcel.2008.01.006>.

Zheng, Y., Liu, B., Wang, L., Lei, H., Zheng, Y., Liu, B., Wang, L., Lei, H., Prieto, K.D.P., and Pan, D. (2017). Homeostatic control of Hpo/MST kinase activity through autophosphorylation-dependent recruitment of the STRIPAK PP2A phosphatase complex. *Cell Rep.* 21, 3612–3623. <https://doi.org/10.1016/j.celrep.2017.11.076>.

Zheng, Y., and Pan, D. (2019). The hippo signaling pathway in development and disease. *Dev. Cell* 50, 264–282. <https://doi.org/10.1016/j.devcel.2019.06.003>.

STAR★METHODS

KEY RESOURCES TABLE

REAGENT or RESOURCE	SOURCE	IDENTIFIER
<b>Antibodies</b>		
mouse anti-Rh5	Gift from C. Desplan	N/A
rabbit anti-Rh6	Gift from C. Desplan	N/A
chicken anti-GFP	Abcam	Cat# ab13970; RRID: AB_300798
mouse anti-Arm	DSHB	Cat# N2 7A1; RRID: AB_528089
rabbit anti-aPKC	Santa Cruz	Cat# sc-208; RRID: AB_2168668
mouse anti-Crb	DSHB	Cat# Cq4; RRID: AB_528181
mouse anti-Dlg	DSHB	Cat# 4F3; RRID: AB_528203
mouse anti- $\alpha$ -Spec	DSHB	Cat# 3A9; RRID: AB_528473
rat anti-Ci	DSHB	Cat# 2A1; RRID: AB_2109711
goat anti-mouse 405	ThermoFisher Scientific	Cat# A31553; RRID: AB_221604
donkey anti-mouse 488	ThermoFisher Scientific	Cat# A21202; RRID: AB_141607
donkey anti-mouse 555	ThermoFisher Scientific	Cat# A31570; RRID: AB_2536180
donkey anti-rabbit 555	ThermoFisher Scientific	Cat# A31572; RRID: AB_162543
donkey anti-rabbit 647	ThermoFisher Scientific	Cat# A31573; RRID: AB_2536183
goat anti-rat 555	ThermoFisher Scientific	Cat# A21434; RRID: AB_2535855
goat anti-chicken 488	ThermoFisher Scientific	Cat# A21449; RRID: AB_2535866
<b>Chemicals, peptides, and recombinant proteins</b>		
Phalloidin-TRITC	Sigma-Aldrich	Cat# P1951
DAPI	Sigma-Aldrich	Cat# D9542
<b>Experimental models: Organisms/strains</b>		
<i>IGMR-Gal4</i>	Gift from C. Desplan	N/A
<i>UAS-<math>\beta</math>-gal RNAi<sup>GD</sup></i>	VDRRC	#51446
<i>UAS-yki RNAi<sup>KK</sup></i>	VDRRC	#104523
<i>UAS-wts RNAi<sup>KK</sup></i>	VDRRC	#106174
<i>UAS-Cka RNAi<sup>GD</sup></i>	VDRRC	#35234
<i>UAS-Cka RNAi<sup>KK</sup></i>	VDRRC	#106971
<i>UAS-Cka RNAi<sup>TRIP.HMS05138</sup></i>	BDSC	#28927
<i>UAS-mts RNAi<sup>TRIP</sup></i>	BDSC	#27723
<i>UAS-Slmap RNAi<sup>TRIP</sup></i>	BDSC	#32509
<i>UAS-Slmap RNAi<sup>GD</sup></i>	VDRRC	#8199
<i>UAS-Rassf RNAi<sup>GD</sup></i>	VDRRC	#21916
<i>UAS-Tao RNAi<sup>GD</sup></i>	VDRRC	#17432
<i>UAS-Tao<sup>d</sup></i>	(Poon et al., 2018)	N/A
<i>UAS-14-3-3<math>\epsilon</math> RNAi<sup>TRIP</sup></i>	BDSC	#34884
<i>UAS-14-3-3<math>\zeta</math> RNAi<sup>TRIP</sup></i>	BDSC	#28327
<i>UAS-mask RNAi<sup>TRIP 1</sup></i>	BDSC	#31574
<i>UAS-mask RNAi<sup>TRIP 2</sup></i>	BDSC	#34571
<i>UAS-mop RNAi<sup>TRIP</sup></i>	BDSC	#32916
<i>UAS-leash RNAi<sup>TRIP</sup></i>	BDSC	#34660
<i>UAS-leash RNAi<sup>GD</sup></i>	BDSC	#26597

(Continued on next page)

**Continued**

REAGENT or RESOURCE	SOURCE	IDENTIFIER
UAS-Hipk RNAi <sup>GD</sup>	VDRC	#32854
UAS-Hipk RNAi <sup>KK</sup>	VDRC	#108254
Wts-Venus	This manuscript	N/A
Hpo-Venus	This manuscript	N/A
Kibra-Venus	(Pojer et al., 2021)	N/A
Mer-Venus	(Pojer et al., 2021)	N/A
Tao-Venus	(Poon et al., 2016)	N/A

**Software and algorithms**

FIJI/ImageJ	(Schindelin et al., 2012)	<a href="https://imagej.net/Fiji">https://imagej.net/Fiji</a>
RStudio	(RStudio Team, 2020)	<a href="http://www.rstudio.com/">http://www.rstudio.com/</a>
ggplot package	(Wickham, 2016)	<a href="https://ggplot2.tidyverse.org/">https://ggplot2.tidyverse.org/</a>
ggbeeswarm package	(Clarke and Sherrill-Mix, 2017)	<a href="https://CRAN.R-project.org/package=ggbeeswarm">https://CRAN.R-project.org/package=ggbeeswarm</a>

**RESOURCE AVAILABILITY**

**Lead contact**

Further information and requests for reagents and data should be directed to the Lead Contact, Kieran Harvey ([kieran.harvey@petermac.org](mailto:kieran.harvey@petermac.org)).

**Materials availability**

*D. melanogaster* lines generated in this study are available from the Lead Contact upon request.

**Data and code availability**

All data reported in this study will be shared by the Lead Contact upon request. This paper does not report original code.

**EXPERIMENTAL MODEL AND SUBJECT DETAILS**

The following *D. melanogaster* stocks were used in this study, many available from the Bloomington *Drosophila* Stock Centre (BDSC) and the Vienna *Drosophila* Resource Centre (VDRC): IGMR-Gal4 (Claude Desplan), UAS-β-gal RNAi<sup>GD</sup> (VDRC, #51446), UAS-yki RNAi<sup>KK</sup> (VDRC, #104523), UAS-wts RNAi<sup>KK</sup> (VDRC, #106174), UAS-Cka RNAi<sup>GD</sup> (VDRC, #35234), UAS-Cka RNAi<sup>KK</sup> (VDRC, #106971), UAS-Cka RNAi<sup>TRIP.HMS05138</sup> (BDSC, #28927), UAS-mts RNAi<sup>TRIP</sup> (BDSC, #27723), UAS-Slmap RNAi<sup>TRIP</sup> (BDSC, #32509), UAS-Slmap RNAi<sup>GD</sup> (VDRC, #8199), UAS-Rassf RNAi<sup>GD</sup> (VDRC, #21916), UAS-Tao RNAi<sup>GD</sup> (VDRC, #17432), UAS-Tao<sup>d</sup> (Poon et al., 2018), UAS-14-3-3ε RNAi<sup>TRIP</sup> (BDSC, #34884), UAS-14-3-3ζ RNAi<sup>TRIP</sup> (BDSC, #28327), UAS-mask RNAi<sup>TRIP 1</sup> (VDRC, #31574), UAS-mask RNAi<sup>TRIP 2</sup> (BDSC, #34571), UAS-mop RNAi<sup>TRIP</sup> (BDSC, #32916), UAS-leash RNAi<sup>TRIP</sup> (BDSC, #34660), UAS-leash RNAi<sup>GD</sup> (VDRC, #26597), UAS-Hipk RNAi<sup>GD</sup> (VDRC, #32854), UAS-Hipk RNAi<sup>KK</sup> (VDRC, #108254), Wts-Venus and Hpo-Venus (this manuscript), Kibra-Venus and Mer-Venus (Pojer et al., 2021), Tao-Venus (Poon et al., 2016).

*D. melanogaster* were raised at room temperature (22-23°C) or 18°C on food made with yeast, glucose, agar and polenta. Animals were fed in excess food availability to ensure that nutritional availability was not limiting. All experiments were carried out at 25°C. Males and females were used for all experiments, unless otherwise specified. For experiments in adult retinas, adults were selected within two days of eclosion. For experiments in pupal eyes, larvae were selected at white prepupae stage (Hsiao et al., 2012), transferred to a petri dish and raised at 25°C for the desired length of time. Venus clones were generated using the *eyFp/FRT* system to generate clones in the *D. melanogaster* eye.

**METHOD DETAILS**

Crosses were carried out at 25°C and tipped into new vials every 2-3 days. An equal number of male and female flies were dissected for each experiment. Dissections were performed as described in Hsiao et al. (2012). Briefly, retinas were dissected in PBS and fixed in 4% paraformaldehyde, washed in PBS for one hour

and rinsed in PBST (PBS with 0.3% Triton X-100). During this wash, the lamina was removed. Retinas with strong pigment were washed in PBST for 4-5 days, with the media refreshed once a day, to remove the pigment. Retinas were blocked in blocking solution (5% NGS in PBST) and incubated overnight in primary antibody at 4°C. Following a one hour wash in PBST, retinas were incubated overnight in secondary antibody at 4°C. Tissues were mounted in VectaShield Mounting Medium (Vector Laboratories, H-1000) or 90% glycerol on bridge slides (Morante and Desplan, 2011). For anti-Crb antibody, tissues were washed in 30% methanol, 50% methanol and 70% methanol for three minutes each, directly after fixation, before continuing with staining as above.

The following primary antibodies were used: mouse anti-Rh5 (1:200, Claude Desplan), rabbit anti-Rh6 (1:1000, Claude Desplan), chicken anti-GFP (1:1000, Abcam, ab13970), mouse anti-Armadillo (1:200, Developmental Studies Hybridoma Bank (DSHB), N2 7A1), rabbit anti-aPKC (1:250, Santa Cruz, sc-208), mouse anti-Crb (1:10, DSHB, Cq4), mouse anti-Dlg (1:50, DSHB, 4F3), mouse anti- $\alpha$ -Spec (1:100, DSHB, 3A9) and rat anti-Ci (1:10, DSHB, 2A1). Secondary antibodies conjugated to Alexa405, Alexa488, Alexa555 and Alexa647 (ThermoFisher Scientific) were used at a concentration of 1:500. DAPI (1:500, Sigma-Aldrich, D9542) and Phalloidin-TRITC (1:200-500, Sigma-Aldrich, P1951) staining was completed before mounting. Images were collected on a Nikon C2 or Olympus FV3000 confocal microscope, or an Olympus FVMPE-RS multiphoton microscope. For experiments examining protein subcellular localisation, at least 5 eyes and 10 R8 cells per eye were examined for each genotype.

## QUANTIFICATION AND STATISTICAL ANALYSIS

Images were analysed using FIJI/ImageJ (Schindelin et al., 2012). All statistical analyses were completed in RStudio (RStudio Team, 2020) using the stats package. All graphs were generated in RStudio using the ggplot (Wickham, 2016) and ggbeeswarm (Clarke and Sherrill-Mix, 2017) packages. The number of R8 cells that expressed Rh5, Rh6 or both, were counted using the FIJI Cell Counter plugin. Retinas were scored only if there were more than 100 ommatidia in a single focal plane and more retinas were imaged or visualised than scored to confirm that the results were consistent. Statistical comparisons between ratios of R8 subtypes was calculated from the total number of Rh5-positive cells (Rh5-positive cells + Rh5- and Rh6-positive cells) using a two-tailed, unpaired t-test with the t.test function, with the following symbols used for p-value cut-offs: \*\*\* < 0.0001, \*\* < 0.001, \* < 0.01, ns > 0.01. Error bars represent the standard deviation.

Quantification of Venus intensity for Venus-tagged proteins was completed after the mean intensity of background in Venus-negative clones was subtracted from the image in FIJI. Statistical comparison of Venus intensity was calculated using an ANOVA and multiple comparisons between stages calculated using Tukey's Honest Significant Difference test, with the following symbols used for p-value cut-offs: \*\*\*\* < 0.0001, \*\*\* < 0.001, \*\* < 0.01, \* < 0.05, ns > 0.05.